Electronic Supporting Information

Potential-Selective Electrochemiluminescence of $AgInS_2$/ZnS Nanocrystals and Its Immunoassay Application

Mengwei Li[a], Xuwen Gao[a], Xiaoxuan Ren[a], Yaojia Ai[a], Bin Zhang[a], Guizheng Zou*[a]*

[a] School of Chemistry and Chemical Engineering, Shandong University, Jinan 250100, PR China

*Corresponding authors E-mail address: zouguizheng@sdu.edu.cn

gaoxuwen@mail.sdu.edu.cn.

Table of Contents

1. Experimental section

1.1 Chemicals and material

All chemical regents are of analytical grade or better, and all aqueous solutions are prepared with double-distilled water (DDW). Indium nitrate hydrate ($In(NO_3)_3 \cdot xH_2O$), sodium sulfide nonahydrate ($Na_2S \cdot 9H_2O$), tripropylamine (TPrA), triethanolamine (TEOA), thioglycolic acid (TGA), 2-(dibutylamino) ethanol (DBAE), bovine serum albumin (BSA), tris(hydroxymethyl)aminomethane (Tris), silver nitrate ($AgNO_3$), 1-hydroxypyrrolidine-2,5-dione (NHS), and *N*-(3-dimethylaminopropyl)-*N*′-ethylcarbodiimide hydrochloride (EDC) are obtained from Aladdin (Shanghai, China). Hydrazine hydrate (N_2H_4), zinc nitrate hexahydrate ($Zn(NO_3)_2 \cdot 6H_2O$), and trisodium citrate (TSC) are obtained from Sinopharm Chemical Reagent Co., Ltd. (Shanghai, China). Potassium ferricyanide ($K_3[Fe(CN)_6]$) and potassium hexacyanoferrate ($K_4[Fe(CN)_6]$) are purchased from Xilong Chemical Co., Ltd. (Shantou, China). Human carcinoembryonic antigen (CEA), primary antibody (Ab_1), and secondary antibody (Ab_2) of CEA, human prostate specific antigen (PSA), human alpha fetoprotein (AFP) and cancer antigen 125 (CA125) are purchased from Beijing Biosynthesis Biotechnology Co., Ltd. (Beijing, China) and diluted with 10 mM pH 7.4 phosphate buffer solution (PBS) before use. Human serum samples are acquired from Qianfoshan Hospital.

1.2 Apparatus and measurements

The ultraviolet-visible (UV–vis) absorption spectrum is measured with a TU-1901 spectrophotometer (Beijing Purkinje General Instrument Co., Ltd., China). The photoluminescence (PL) spectrum is recorded on an F-320 spectrofluorimeter (Tianjin Gangdong Sci. &Tech. Development Co., Ltd., China). The PL quantum yield (PLQY) is measured with a FLS920 fluorescence spectrometer (Edinburgh Instruments, U.K.). High-resolution transmission electron microscopy (HRTEM) image is taken on a Talos F200X G2 transmission electron microscopy with an intermediate acceleration voltage of 300 kV (Thermo Fisher Scientific Co., Ltd., USA). X-ray diffraction (XRD) pattern

is recorded using an X-ray diffractometer (Bruker AXS D8 Advance, Germany) with Cu Kα radiation (λ = 1.5418 Å). Fourier transform infrared spectroscopy (FT-IR) spectrum is recorded on an ALPHA II Fourier Transform Infrared spectrometer (Bruker Co., Ltd, Germany). Zeta potential (ζ) is measured on a NanoZS Zetasizer Nanoseries (Malvern Instruments Ltd). X-ray photoelectron spectroscopy (XPS) is performed with Thermo Scientific K-Alpha (Thermo Fisher Scientific Co., USA) using monochromatic Al Kα radiation. Differential pulse voltammetry (DPV) is recorded on a CHI 1040C electrochemical analyzer (Shanghai, China). Linear sweep voltammetry (LSV), cyclic voltammetry (CV), and ECL-potential profiles are recorded on MPI-II ECL analyzer (Xi'an Remex Analytical Instrument Co., Ltd, China) using a three-electrode system including a 5 mm diameter working electrode, a Pt counter electrode, and an Ag/AgCl (saturated KCl) reference electrode. ECL spectra are obtained on GCFG-B ECL spectrum analyzer (Shandong GuoChen Biotech Co., Ltd., China).

1.3 Preparation of AIS/ZnS NCs

The $AgInS_2$/ZnS (AIS/ZnS) nanocrystals (NCs) is synthesized according to the previously reported procedure with modification.[1] $AgNO_3$ (0.05 mmol), $In(NO_3)_3$ (0.2 mmol), TSC (0.4 mmol), TGA (0.05 mmol) and Na_2S (0.3 mmol) are added into 50 mL DDW in sequence under vigorously stirring, and kept at 100 ℃ for 20 min to obtain AIS core. Then, an 8 mL aqueous solution containing 1 mmol TSC and 0.8 mmol $Zn(NO_3)_2$ and 1 mL aqueous solution containing 0.2 mmol Na_2S are slowly introduced into the mixture. The final mixture is kept at 100 ℃ for 2 h to form AIS/ZnS NCs. The obtained AIS/ZnS NCs is purified with isopropyl alcohol via centrifugation at 12000 rpm, and the purified AIS/ZnS NCs is re-dispersed in DDW.

1.4 Preparation of AIS/ZnS NCs labeled Ab_2 (i.e., Ab_2|AIS/ZnS)

As demonstrated in Scheme S1A, the Ab_2|AIS/ZnS conjugates are prepared with the assistance of EDC and NHS. The carboxylic groups of AIS/ZnS NCs are activated by mixing 500 μL 1 mg/mL AIS/ZnS NCs with 10 μL of pH 6.0 PBS (10 mM) containing 100 mg/mL EDC and 100 mg/mL NHS for 30 min at 37 ℃. The AIS/ZnS NCs are collected via centrifugation and then re-dispersed into a drop of 500 μL of 10 mM pH

7.4 PBS. 100 μL of 10 μg/mL Ab_2 is injected into the obtained solution and incubated at 37 ℃ to form Ab_2|AIS/ZnS conjugates. 3 h later, 10 μL of 1% (v/v) BSA is introduced into the mixed solution to block the nonspecific binding sites of conjugates for 30 min. Finally, the Ab_2|AIS/ZnS conjugates are purified three times via centrifugation, re-dispersed in 500 μL of 10 mM pH 7.4 PBS, and stored at 4 ℃ for further use.

1.5 Fabrication of ECL immunosensor.

As demonstrated in Scheme S1B, Au electrode is polished with 0.3 μm alumina slurry, and then soaked in 10 mM MPA solution for 10 h to form Au|MPA. The carboxyl groups of Au|MPA are activated with 20 μL of 100 mg/mL EDC and 100 mg/mL NHS for 1 h. Then the Au|MPA is incubated with 10 μL of 10 μg/mL Ab_1 at 37 ℃ for 1 h to form Au|MPA-Ab_1. Au|MPA-Ab_1 is rinsed with 10 mM 7.4 PBS and incubated with 10 μL 1% (v/v) BSA solution for 30 min to block nonspecific adsorption sites. Au|MPA-Ab_1 is incubated with 10 μL of CEA with different concentrations for 30 min at 37 ℃ to form Au|MPA-Ab_1<CEA. Au|MPA-Ab_1<CEA is further incubated with 10 μL of Ab_2|AIS/ZnS at 37 ℃ for 1 h to obtain Au|MPA-Ab_1<CEA>Ab_2|AIS/ZnS.

2. Results and discussion

2.1 Schematic illustration for the ECL immunosensor

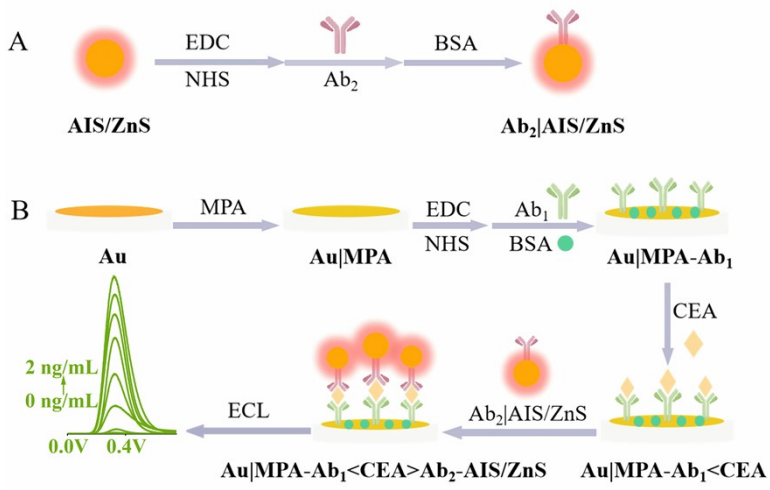

Scheme S1 Schematic illustration for the preparation of (A) Ab_2|AIS/ZnS and (B) the ECL sensor for CEA detection by using AIS/ZnS NCs as tag.

2.2 UV−vis absorption and PL spectra of AIS/ZnS NCs

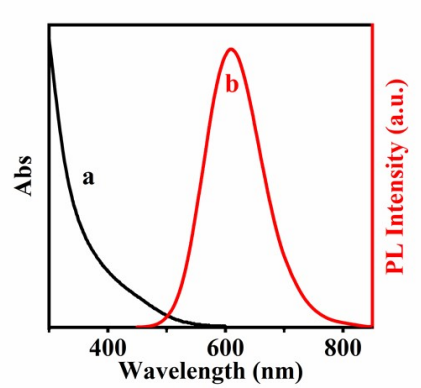

Fig. S1 UV−vis absorption (a, black line) and PL (b, red line, λ_{ex} = 420 nm) spectra of 1.0 mg/mL AIS/ZnS NCs in DDW.

2.3 HRTEM image of AIS/ZnS NCs

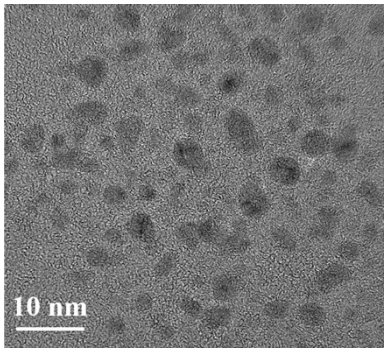

Fig. S2 HRTEM image of AIS/ZnS NCs.

2.4 XRD pattern of AIS/ZnS NCs

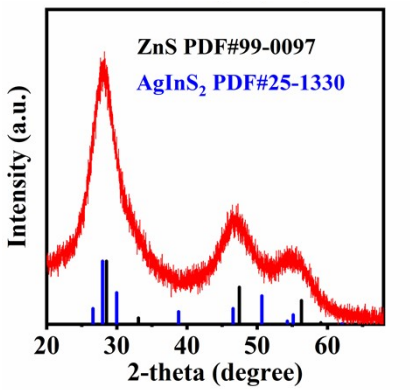

Fig. S3 XRD pattern of AIS/ZnS NCs.

2.5 XPS spectrum of AIS/ZnS NCs

Fig. S4 XPS spectrum of AIS/ZnS NCs.

2.6 Zeta potential profile of AIS/ZnS NCs

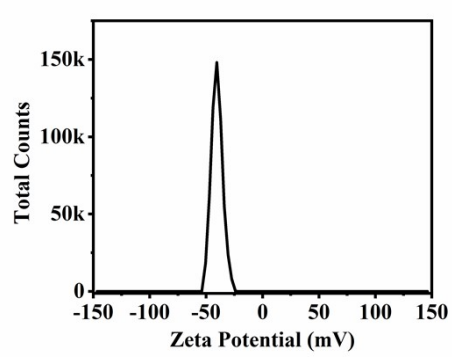

Fig. S5 Zeta potential profile of monodispersed AIS/ZnS NCs in DDW.

2.7 FT-IR spectrum of AIS/ZnS NCs

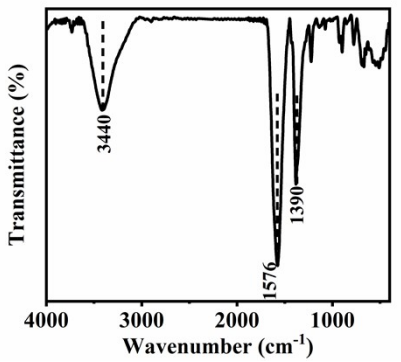

Fig. S6 FT-IR spectrum of AIS/ZnS NCs.

2.8 The ECL maximum-emission-potential of AIS/ZnS NCs

Table S1 The ECL maximum-emission-potential of AIS/ZnS NCs on different electrodes with different co-reactants.

Co-reactant / ECL-potential / Electrode	N_2H_4	TPrA	DBAE	TEOA
Au	0.30 V	0.86 V	0.89 V	0.86 V
Pt	0.80 V	0.91 V	0.85 V	0.80 V
GCE	0.95 V	0.92 V	0.91 V	0.83 V

2.9 DPV profiles of AIS/ZnS NCs on Pt electrode and GCE

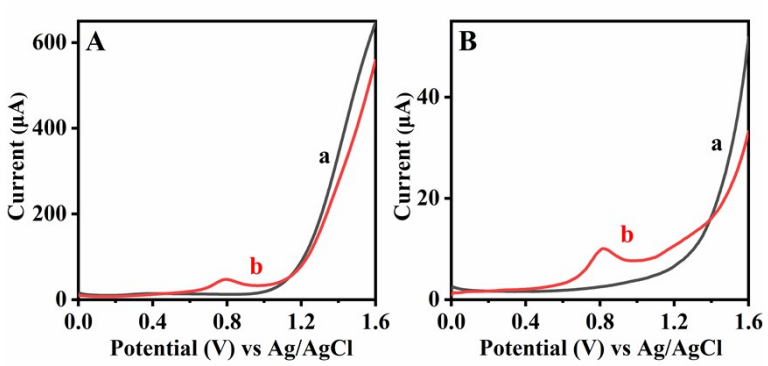

Fig. S7 DPV profiles of (A) Pt electrode and (B) GCE in (a) 0.1 M pH 7.4 Tris-HCl and (b) a + 1.0 mg/mL AIS/ZnS NCs.

2.10 The characterization of Ab_2|AIS/ZnS

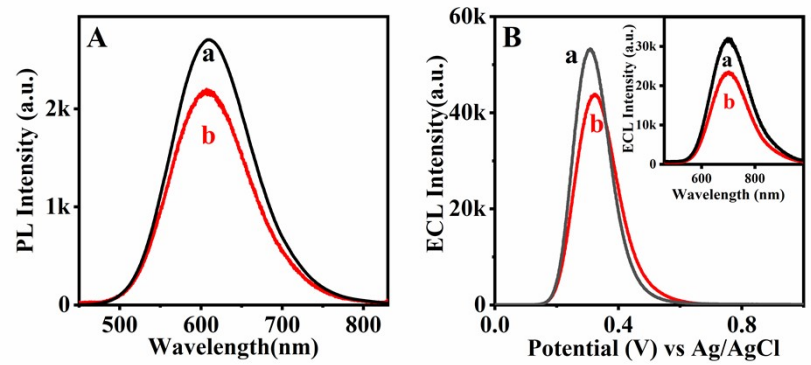

Fig. S8 (A) PL (λ_{ex} = 420 nm) spectra of 1.0 mg/mL AIS/ZnS NCs (a, black line) and 1.0 mg/mL Ab_2|AIS/ZnS (b, red line) in DDW, respectively. (B) ECL intensity-potential profiles of 1.0 mg/mL AIS/ZnS NCs (a, black line) and 1.0 mg/mL Ab_2|AIS/ZnS (b, red line) in 0.1 M pH 7.4 Tris-HCl containing 10 mM N_2H_4 and 1.0 mg/mL Ab_2|AIS/ZnS by scanning Au electrode from 0 to +1.0 V at 50 mV/s, respectively. Inset of B: corresponding ECL spectra of AIS/ZnS NCs (a, black line) and

Ab_2|AIS/ZnS (b, red line).

As shown in Fig. S8, PL and ECL of Ab_2|AIS/ZnS conjugates are lowered than AIS/ZnS NCs, which probably due to that Ab_2 within the conjugates would hinder the hole (or electron) injecting process occurred at AIS/ZnS NCs surface.[2] The ECL intensity-potential and spectral profiles of AIS/ZnS NCs and Ab_2|AIS/ZnS conjugates are similar with each other. It is clear that both the PL and ECL natures of AIS/ZnS NCs are primarily preserved in the Ab_2|AIS/ZnS conjugates..

2.11 Fabricating characterization of ECL immunosensor

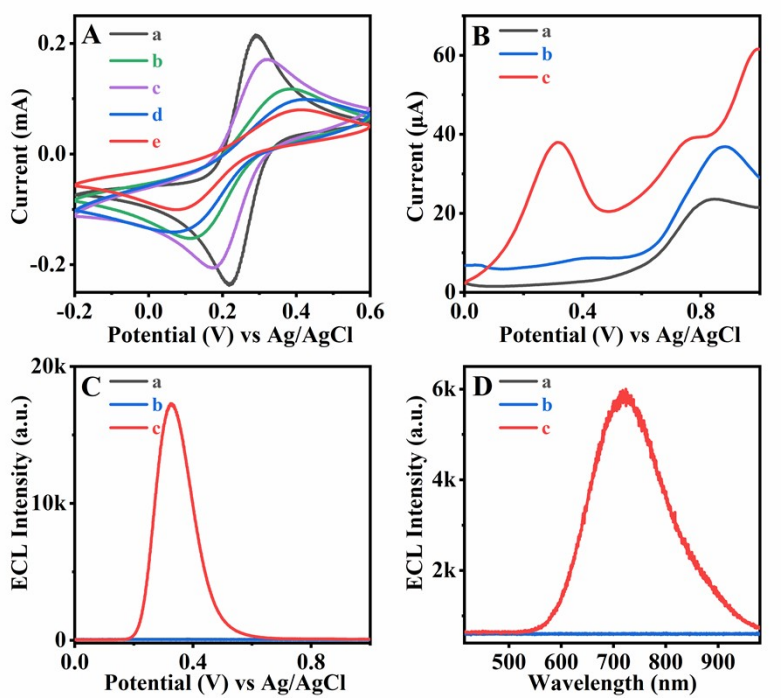

Fig. S9 (A) CV profiles of (a) Au, (b) Au|MPA, (c) Au|MPA-Ab_1, (d) Au|MPA-Ab_1<CEA, and (e) Au|MPA-Ab_1<CEA>Ab_2|AIS/ZnS in 0.1 M KCl solution containing 5 mM $K_3Fe(CN)_6$ and 5 mM $K_4Fe(CN)_6$. (B) DPV profiles of (a) Au, (b) Au|MPA-Ab_1<CEA, and (c) Au|MPA-Ab_1<CEA>Ab_2|AIS/ZnS in 0.1 M pH 7.4 Tris-HCl by scanning the potential from 0 to +1.0 V at 50 mV/s. (C) ECL intensity-potential profiles and (D) accumulated ECL spectra of (a) Au, (b) Au|MPA-Ab_1<CEA, and (c) Au|MPA-Ab_1<CEA>Ab_2|AIS/ZnS in 0.1 M pH 7.4 Tris-HCl containing 10 mM N_2H_4 by scanning the potential from 0 to +1.0 V at 50 mV/s. The concentration of CEA is 50 pg/mL.

As shown in Fig. S9A, Au electrode shows a pair of reversible redox peaks with a peak potential difference of ~70 mV (curve a). After fixing MPA to Au electrode via forming Au-S bond, the current decreases and the peak potential difference increases (curve b) due to the electrostatic repulsion between the deprotonated carboxyl group of

Au|MPA and the negatively charged $Fe(CN)_6^{3-}/Fe(CN)_6^{4-}$.[3] Au|MPA-$Ab_1$ exhibits partially restored current, indicating the decreased negative charge on electrode surface upon labeling Ab_1 onto Au|MPA (curve c). Au|MPA-Ab_1<CEA (curve d) and Au|MPA-Ab_1<CEA>Ab_2|AIS/ZnS (curve e) show further decreased peak current and increased peak potential separation in sequence, because the surface-confined biomacromolecules on the electrode usually hinder the redox of $Fe(CN)_6^{3-}/Fe(CN)_6^{4-}$.[4] All these data indicate that AIS/ZnS NCs is immobilized on Au surface via the proposed immunosensor fabricating procedure.

As shown in Fig. S9B-9D, the surface-confined AIS/ZnS NCs in Au|MPA-Ab_1<CEA>Ab_2|AIS/ZnS not only displays a distinct oxidation process around 0.31 V (Fig. S9B), indicating the low oxidative potential nature of AIS/ZnS NCs is primarily preserved in the ECL immunosensor, but also exhibits an obvious ECL process with the maximum emission potential around 0.32 V when employing N_2H_4 as co-reactant, manifesting the low-triggering-potential ECL of AIS/ZnS NCs is preserved in the immunocomplexes. ECL of Au|MPA-Ab_1<CEA>Ab_2|AIS/ZnS is located around 722 nm, red-shifted for 22 nm to that of AIS/ZnS NCs (Fig. S9D).

2.12 Comparison of the performance of different sensors for CEA determination

Table S2 Comparison of the performance of different sensors for CEA determination.

Lables	Method	Linear range	LOD	Ref
MXC-Fe_3O_4-Ru	DPV	1 pg/mL − 1 μg/mL	0.62 pg/mL	[5]
Lable-free	CL	0.1 ng/mL − 60 ng/mL	0.05 ng/mL	[6]
Lable-free	ECL	-	1 pg/mL	[7]
CdTe NCs	ECL	10 pg/mL – 10 ng/mL	1 pg/mL	[8]
AIS/ZnS NCs	ECL	0.5 pg/mL − 500 pg/mL	0.2 pg/mL	This work

2.13 Stability of ECL sensor for CEA assay

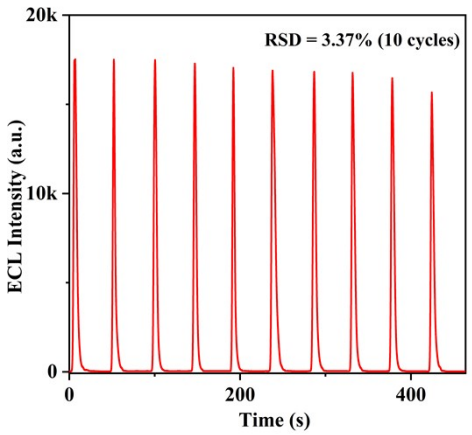

Fig. S10 The ECL stability of Au|MPA-Ab$_1$<CEA>Ab$_2$|AIS/ZnS toward 50 pg/mL CEA by scanning the potential from 0 to +1.0 V for 10 cycles.

As shown in Fig. S10, ECL response of the proposed sensor is efficient and stable enough with the relative standard deviation (RSD) of 3.37%.

2.14 Real-sample analysis of CEA

Table S3 Real-sample analysis of CEA in human serum (n = 3).

Number	Standard amount (pg/mL)	Detected amount (pg/mL)	RSD (%)	Recovery (%)
1	10	10.31	2.24	103.1
2	50	50.29	2.22	100.6
3	200	192.27	4.93	96.1

Three serum samples, which are obtained from Qianfoshan Hospital with CEA of a concentration beyond the calibration curve of Au|MPA-Ab$_1$<CEA>Ab$_2$|AIS/ZnS, are respectively diluted to 10.0, 50.0, and 200.0 pg/mL levels. According to Table S3, final concentration of the diluted samples is determined to be 10.31, 50.29, and 192.27 pg/mL (n = 3), respectively, which indicates that the accuracy of CEA assay in real sample is acceptable.

Notes and references

1 M. D. Regulacio, K. Y. Win, S. L. Lo, S. Y. Zhang, X. H. Zhang, S. Wang, M. Y. Han and Y. G. Zheng, *Nanoscale*, 2013, **5**, 2322–2327.

2 X. Zhang, X. Tan, B. Zhang, W. J. Miao and G. Z. Zou, *Anal. Chem.*, 2016, **88**, 6947-6953.

3 L. Fu, X. W. Gao, S. T. Dong, H. Y. Hsu and G. Z. Zou, *Anal. Chem.*, 2021, **93**, 4909–4915.

4 X. W. Gao, X. X. Ren, Y. J. Ai, M. W. Li, B. Zhang and G. Z. Zou, *Anal. Chem.*, 2023, **95**, 6948–6954.

5 H. Q. Yang, Y. Xu, Q. Q. Hou, Q. Z. Xu and C. F. Ding, *Biosens. Bioelectron.*, 2022, **208**, 114216.

6 J. Li, Y. Cao, S. S. Hinman, K. S. McKeating, Y. W. Guan, X. Y. Hu, Q. Cheng and Z. J. Yang, *Biosens. Bioelectron.*, 2018, **100**, 304–311.

7 J. J. Zhang, R. Jin, D. C. Jiang and H. Y. Chen, *J. Am. Chem. Soc.*, 2019, **141**, 10294–10299.

8 G. Z. Zou, X. Tan, X. Y. Long, Y. P. He and W. J. Miao, *Anal. Chem.*, 2017, **89**, 13024–13029.